ARTICLE

Electron Momentum Distributions for $4a_1$ Orbitals of CF_xCl_{4-x} in Low Momentum Region: a Possible Evidence of Molecular Geometry Distortion[†]

Xu Shan, Chun-kai Xu, Xiao-feng Yin, Li-xia Zhou, Ke-zun Xu, Xiang-jun Chen*

Hefei National Laboratory for Physical Sciences at Microscale and Department of Modern Physics, University of Science and Technology of China, Hefei 230026, China

(Dated: Received on August 27, 2009; Accepted on September 25, 2009)

Electron momentum distributions for $4a_1$ orbitals of serial freon molecules CF_3Cl, CF_2Cl_2, and $CFCl_3$ (CF_xCl_{4-x}, x=1−3) have been reanalyzed due to the severe discrepancies between theory and experiment in low momentum region. The tentative calculations using equilibrium geometries of molecular ions have exhibited a great improvement in agreement with the experimental data, which suggests that the molecular geometry distortion may be responsible for the observed high intensities at p<0.5 a.u.. Further analyses show that the severe discrepancies at low momentum region mainly arise from the influence of molecular geometry distortion on C−Cl bonding electron density distributions.

Key words: (e, 2e), Electron momentum spectroscopy, Molecular geometry distortion, Electron density distribution

I. INTRODUCTION

Electron momentum spectroscopy (EMS), which is particularly sensitive to the chemically important low momentum (outer spatial) electron density of valence orbitals, has become one of premier tools in the study of electronic structure of atoms and molecules due to its unique ability to directly obtain spherically averaged electron density distribution of individual orbital in momentum space [1−5]. The low momentum component of electron density distributions for valence orbitals has always been an interesting focus and attracted extensive attention of many researchers. In the previous EMS studies, large discrepancies between experimental and theoretical electron density distributions in low momentum region have been observed for a lot of atomic and molecular orbitals [6−21]. Several possible reasons have been proposed in attempt to explain these discrepancies. One possible cause is the distorted wave effect at low momentum region proposed by Brion *et al.* to explain the observed high intensity in electron momentum distributions of a series of atomic d orbitals, which is due to the high angular momentum effect and the even-parity nature of atomic d orbitals [6]. This interpretive model have been extended to explain the observed high intensity at low momentum region for a lot of atomic d-like or π^*-like molecular orbitals that exhibit gerade type symmetry [6−11].

Another possible cause is the change of molecular geometry at the instant of ionization, which was put forth by Tossell *et al.* to explain the experimental high intensity at low momentum region relative to the calculation in neutral molecular geometry (D_{3h}) for the $3e'$ orbital of cyclopropane [12]. Based on their further calculations employing two distorted cationic geometries (C_{2v}), Tossell *et al.* suggested the large intensity observed in their experiment should be attributed to the case that the orbital electron momentum distribution varies in response to a change of molecular geometry [12]. However, the subsequent EMS experiment of Banjavčić *et al.* with better energy and momentum resolutions (1.4 eV and 0.12 a.u. respectively) showed almost zero intensity at $p\approx0$ for the $3e'$ orbital of cyclopropane [13], which indicates that the high intensity observed by Tossell *et al.* should be due to the poor momentum resolution (∼0.28 a.u.) [12]. Goruganthu *et al.* have also applied this model to explain the similar high density at small momentum for the outermost occupied orbital of 2-butyne [14], and only a finite improvement has been achieved in amplitude of the momentum density at low momentum region. Moreover, in order to explain the observed large momentum density in low momentum region for valence orbitals of water, Leung *et al.* have carried out a more detailed calculation by considering vibrational averaging effects, but no obvious improvement has been obtained [15]. Later, Hollebone *et al.* investigated the vibrational effects on $1b_{3u}$ orbital of ethylene and pointed out the vibrational effects are very small and do not significantly change the shape of electron momentum distributions [16]. For the case of water molecule, the high-quality calculation of Bawagan *et al.* using the configuration-interaction method (CI)

[†]Part of the special issue for "the Chinese Chemical Society's 11th National Chemical Dynamics Symposium".

*Author to whom correspondence should be addressed. E-mail: xjun@ustc.edu.cn

[17] and that of Duffy *et al.* using Kohn-Sham density-functional theory (DFT) showed that the observed high intensity in low momentum region for valence orbitals of water should be ascribed to the strong electron correlation effects [18]. Recently, ultrafast nuclear dynamical processes, *i.e.*, molecular geometry distortion (or relaxation) and vibronic coupling interactions in a molecule, have been invoked in order to explain a strong rise of electron density distributions at low momentum region in the latest EMS studies [19,20].

However, up to now, the origin of the dramatic discrepancies between theoretical and experimental electron density distributions in low momentum region still remains vague. Thus, it is of significance to identify the origin by further extensive and comparative investigations. Interestingly, our recent EMS studies [21−23] on a series of molecules CF_3Cl, CF_2Cl_2, and $CFCl_3$ (CF_xCl_{4-x}, x=1−3) have also displayed large discrepancies between experimental and theoretical electron momentum distributions for $4a_1$ orbitals in low momentum region. The possibility of some experimental artifact is ruled out on the experimental side because of the almost identical results for CF_2Cl_2 molecule measured independently by Chen *et al.* [22], Ning *et al.* [24], and Shan *et al.* [25] using three different EMS spectrometers with different experimental conditions. Likewise, the almost identical results for outer valence orbitals of CF_2Cl_2 obtained from three independent experiments at the impact energies of 1.2 and 2.5 keV suggest that plane wave impulse approximation was valid, and the distorted wave effect might be excluded, at least, not a primary factor responsible for the observed large discrepancies for $4a_1$ orbitals in low momentum region. As for electron correlation effects that might also be contributed to the high intensity in low momentum [17], we have carried out the calculations employing DFT-B3LYP method and larger basis sets approaching to saturation and found that the large differences between calculations and experiments still remain. Noting that the quality of the DFT calculations has been proved to be comparable to that of CI method for many molecules [18,26−31], the electron correlation and basis sets effects could be excluded. Therefore, in present study, we concentrate on the viewpoint of molecular geometry distortion and try to explore the origin of the large discrepancies between experiment and theory for $4a_1$ orbitals of CF_xCl_{4-x} compounds at low momentum region.

II. EXPERIMENTS AND THEORETICS

The details of the present EMS spectrometer have been given elsewhere [32] and thus only a brief description will be given here. The gas phase target molecule is ionized by an impact with a high-energy electron beam (E_0=E_b+1.2 keV, which E_b is binding energy). The scattered and ejected electrons are received by two hemispherical electron energy analyzers with a five-element cylindrical retarding lens and detected in coincidence by one-dimensional position sensitive detectors. In the symmetric non-coplanar geometry, the two outgoing electrons have essentially the equal energy and the same polar angles (θ_1=θ_2=45°). The relative azimuthal angle ϕ between two outgoing electrons is variable over wide range from −30° to 30° by rotating one analyzer around the incident electron beam and keeping the other one fixed. In such a condition, using the plane wave impulse approximation, the EMS differential cross-section ($\sigma_{\rm EMS}$) for randomly oriented gas-phase molecule at a given binding energy is proportional to the squared form factor $F_{if}(\mathbf{p})$ which is given by

$$F_{if}(\mathbf{p}) = \langle \mathbf{p}\Psi_f(\tau,Q)|\Psi_i(\mathbf{r},\tau,Q)\rangle \tag{1}$$

where $\Psi_i(\mathbf{r},\tau,Q)$ and $\Psi_f(\tau,Q)$ are wavefunctions for the molecule and the residual ion respectively. And the quantity $\mathbf{p}$ is the momentum of the target electron prior to knockout. Q denotes the set of coordinates determining the displacements from equilibrium of atomic nuclei of molecule, $\mathbf{r}$ is the coordinates of the ejected electron in lab system, and τ is the set of coordinates of the remaining $Z-1$ electrons.

With the Born-Oppenheimer approximation, disregarding the coupling between the rotational and internal motion of a molecule, the wavefunctions Ψ_i and Ψ_f can be represented as the products of the electronic (ψ_n), vibrational (X_{nv}), and rotational (Φ_{JMK}) functions. Thus, Eq.(1) can be written as

$$\begin{aligned} F_{if}(\mathbf{p}) = &\langle \Phi_{J'M'K'}(\Omega)X_{n'\nu'}(Q)\mathbf{p}\psi_{n'}(\tau,Q)|\cdot \\ &\psi_n(\mathbf{r},\tau,Q)X_{n\nu}(Q)\Phi_{JMK}(\Omega)\rangle \end{aligned} \tag{2}$$

where Ω is Euler angle determining the molecule orientation in space.

The integral of electronic part in Eq.(2) was reduced by Levin *et al.* to the following form [33]

$$\langle \mathbf{p}\psi_{n'}(\tau,Q)|\psi_n(\mathbf{r},\tau,Q)\rangle = S_{nn'}(Q)\varphi_\gamma(\mathbf{p},Q) \tag{3}$$

where $S_{nn'}(Q)$ is the overlap integral of the wavefunctions for the final ion and molecular residue left after the knockout of an electron from the one-electron molecular orbital $\varphi_\gamma(\mathbf{p},Q)$ in momentum space.

Taking into account of Eq.(3), the integral over vibrational coordinates in Eq.(2) was further reduced to the following form [33]

$$\begin{aligned} &\langle X_{n'\nu'}(Q)|S_{nn'}(Q)\varphi_\gamma(\mathbf{p},Q)X_{n\nu}(Q)\rangle \\ &= g_{n\nu}^{n'\nu'}S_{nn'}(\overline{Q})\varphi_\gamma(\mathbf{p},\overline{Q}) \end{aligned} \tag{4}$$

where $g_{n\nu}^{n'\nu'}$=$\langle X_{n'\nu'}(Q)|X_{n\nu}(Q)\rangle$ is the usual Frank-Condon factor, and $\overline{Q}$ corresponds to some mean values of nuclear coordinates intermediate between the equilibrium coordinates of nuclei Q_0 and Q_0' in the initial molecule and in the final molecular ion, respectively. Estimates made by Levin *et al.* for light diatomic

DOI:10.1088/1674-0068/22/06/642-648

TABLE I Equilibrium geometries of CF_xCl_{4-x} and $CF_xCl_{4-x}{}^+$ optimized by B3LYP method with 6-311++G** basis set.

Molecules/ions	Bond lengths/Å		Bond angles/(°)	
	R(C−F)	R(C−Cl)	∠F−C−F	∠Cl−C−Cl
CF_3Cl/CF_3Cl^+	1.333/1.257	1.773/2.390	108.6/117.9	
$CF_2Cl_2/CF_2Cl_2{}^+$	1.338/1.290	1.779/1.823	107.8/113.0	112.1/ 93.4
$CFCl_3/CFCl_3{}^+$	1.344/1.308	1.784/1.780		110.9/108.4

molecules showed that the value $S_{nn'}(Q)\varphi_\gamma(\mathbf{p},Q)$, which is entirely determined by the electron part of the wavefunctions, slowly varies in the range of Q values between Q_0 and $Q_0^{'}$ [33]. Therefore, in EMS studies, the $\overline{Q}$ value in the calculation is usually chosen as the equilibrium coordinates of nuclei Q_0 in the initial molecule. In addition, because the vibrational and rotational states are not resolved by present electron momentum spectrometer, the EMS cross section can be enormously simplified using the closure relations and given as

$$\sigma_{\rm EMS} \propto |S_{nn'}(\overline{Q})|^2 \int |\varphi_\gamma(\mathbf{p},\overline{Q})|^2 {\rm d}\Omega_{\mathbf{p}} \qquad (5)$$

The integral in the Eq.(5) is known as the spherically averaged one-electron momentum distribution, and $|S_{nn'}(\overline{Q})|^2$ corresponds to the pole strength. In the further target Hartree-Fock approximation (THFA) [1] or target Kohn-Sham approximation (TKSA) [18], the wavefunction $\varphi_\gamma(\mathbf{p},\overline{Q})$ can be approximately replaced by the one-electron momentum space canonical HF or KS orbital wavefunction.

In this work, as an attempt to explain the large discrepancies between experimental and theoretical electron momentum distributions for $4a_1$ orbitals of CF_xCl_{4-x} in the low momentum region, we have respectively chosen the neutral and cationic equilibrium geometries (*i.e.* Q_0 and $Q_0^{'}$) in the calculations of spherically averaged electron momentum distributions using TKSA because the stringent calculation of the overlap integral in Eq.(4) between neutral and ionic wavefunctions including electronic and vibrational functions is very difficult at present theoretical stage. The B3LYP functional method with 6-311++G** basis set in the Gaussian 98 package program [34] was employed to optimize neutral and ionic equilibrium geometries and to calculate position space Kohn-Sham orbital wave functions. Much larger basis set of aug-cc-pVTZ has been also used in the calculations but the results show small changes compared with 6-311++G** indicating the basis set approaches to saturation. Therefore only the 6-311++G** calculations will be given in next section.

III. RESULTS AND DISSCUSSION

A. Equilibrium geometries of neutral molecules and the corresponding cations

The equilibrium geometry optimizations of CF_xCl_{4-x} molecules and the corresponding molecular cations have been performed using B3LYP/6-311++G**. The computed structures for the neutral and cationic species are given in Table I. It can be seen that there are large differences on bond distances and bond angles in the neutral and corresponding cationic equilibrium geometries. For CF_3Cl/CF_3Cl^+ system, ionization of an electron makes C−F bond length shorten by 0.076 Å, C−Cl bond length elongate by 0.617 Å and ∠F−C−F increase by 9.3° relative to the neutral molecule. The case of $CF_2Cl_2/CF_2Cl_2{}^+$ system is similar to that of the CF_3Cl/CF_3Cl^+ system. Relative to the neutral molecule, C−F bond length shortens by 0.048 Å and C−Cl bond length increases by 0.044 Å, and ∠F−C−F increases by 5.2° while Cl−C−Cl bond angle largely decreases by 18.7°. Whereas, for $CFCl_3/CFCl_3{}^+$ system, C−F bond and C−Cl bond lengths decrease by 0.036 and 0.004 Å respectively, and the ∠Cl−C−Cl decreases by 2.5° relative to the neutral molecule.

B. Experimental and theoretical electron momentum profiles

The $4a_1$ orbitals of CF_xCl_{4-x} are too close to the adjacent orbitals to be separately resolved by EMS spectrometer. Thus, only the summed Experimental Momentum Profiles (XMPs) and Theoretical Momentum Profile (TMPs) for $4a_1$ and 2e (for CF_3Cl, $CFCl_3$) or $2b_1$, $2b_2$ (for CF_2Cl_2) are shown in Figs.1−3, together with corresponding TMPs for individual orbital respectively. In order to have a stringent comparison of theory and experiment, the instrumental momentum resolution of 0.15 a.u. has been folded into the TMPs and the experimental and theoretical results are normalized to a common intensity scale using $4\pi \int |\varphi_\gamma|^2 p^2 {\rm d}p$=1.

As shown in Fig.1(a), Fig.2(a), and Fig.3(a), the summed TMPs well reproduce the experimental results at p>0.5 a.u. But, at low momentum region of p<0.5 a.u., the TMPs calculated in the neutral geometry (the solid curves) have largely underestimated the experimental intensity, while the results calculated in the cationic geometry (the dashed curves) have obtained obvious improvements. It indicates that the change of molecular geometry has an important influence on orbital electron momentum distributions, especially in the low momentum region. In other words, for the present CF_xCl_{4-x} system, the change of the value $S_{nn'}(Q)\varphi_\gamma(\mathbf{p},Q)$ in the range of Q values between Q_0

DOI:10.1088/1674-0068/22/06/642-648

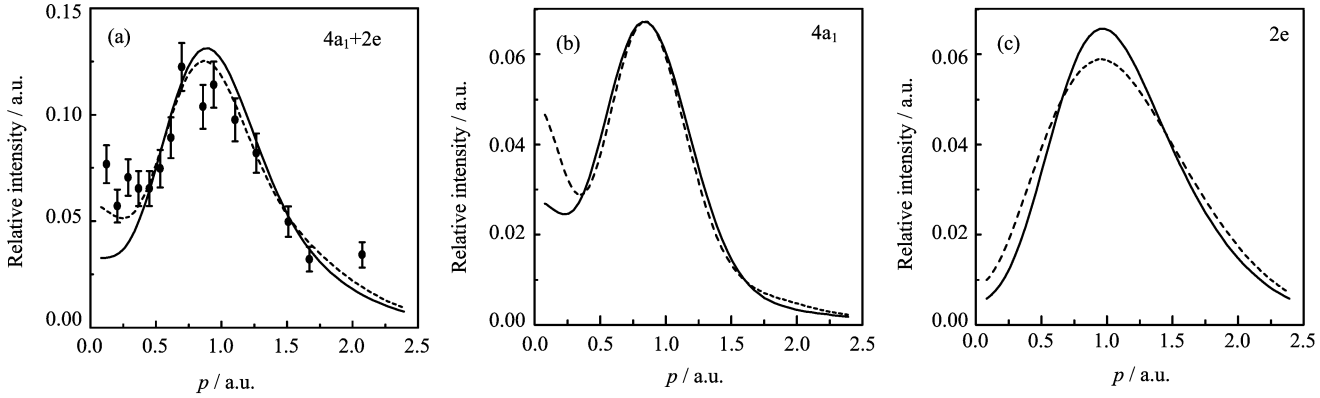

FIG. 1 Experimental and theoretical momentum profiles for the sum of 2e and $4a_1$ orbitals of CF_3Cl, together with the TMPs for individual orbital. Experiment of this work (•), B3LYP/6-311++G** TMPs for neutral (solid line), and cationic (dashed line) geometry.

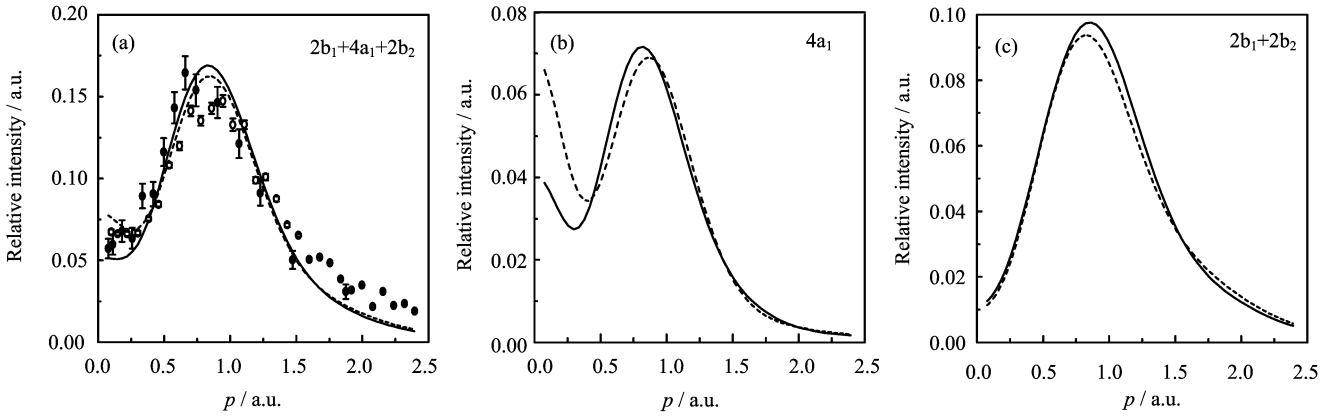

FIG. 2 Experimental and theoretical momentum profiles for the sum of $2b_1$, $2b_2$, and $4a_1$ orbitals of CF_2Cl_2, together with the TMPs for individual orbital. Experiment of this work (•), experiment of Ref.[24] (○), B3LYP/6-311++G** TMPs for neutral (solid line), and cationic (dashed line) geometry.

and $Q_0^{'}$ may not be slow, unlike the estimates made by Levin *et al.* for light diatomic molecules [33]. It is probably not suitable to choose the $\overline{Q}$ value as the equilibrium coordinates of nuclei Q_0 of the initial molecule in the calculation of TMPs.

In addition, it can be seen from Fig.1 (b) and (c), Fig.2 (b) and (c), Fig.3 (b) and (c) that electron momentum profiles of 2e orbital or $2b_1$ and $2b_2$ orbitals calculated in neutral geometries are almost the same as those in cationic geometries. Whereas, the low momentum results of $4a_1$ orbitals have displayed a large difference in the neutral and ionic geometries. Thus, the high intensity of the summed electron momentum profiles in the low momentum region mainly comes from the contribution of $4a_1$ orbitals, rather than 2e, $2b_1$, and $2b_2$ orbitals. Furthermore, electron momentum profiles of $4a_1$ orbitals exhibit a mixture of s-type and p-type character. According to the molecular orbital theory, the s-type character of $4a_1$ orbital electron momentum profile should arise from the s-component of orbital wavefunctions. So the observed high intensity in the low momentum region should be ascribed to the influence of the molecular geometry change on the s-component of $4a_1$ orbital wavefunctions.

C. Theoretical electron density contour maps for the neutral and ionic geometries

In order to further analyze the effect of molecular geometry distortion on electron density distributions, the electron density contour maps in position space of $4a_1$ orbitals calculated in the neutral and cationic geometries are given in Fig.4. It can be seen that $4a_1$ orbital of CF_3Cl is mainly C−F π-bond, which comes from the contribution of C2p and F2p, together with the weak C−Cl σ-bond (mainly Cl3s). For CF_2Cl_2 molecule, $4a_1$ orbital is mainly C−F π-bond (C2p and F2p) and C−Cl σ-bond (C2p and Cl3s). While $4a_1$ orbital of $CFCl_3$ molecule is mainly C−F σ-bond (C2p and F2p) and C−Cl σ-bond (C2p and Cl3s). Above analyzed characters of chemical bonding for $4a_1$ orbitals of CF_xCl_{4-x} molecules are of agreement with those pre-

DOI:10.1088/1674-0068/22/06/642-648

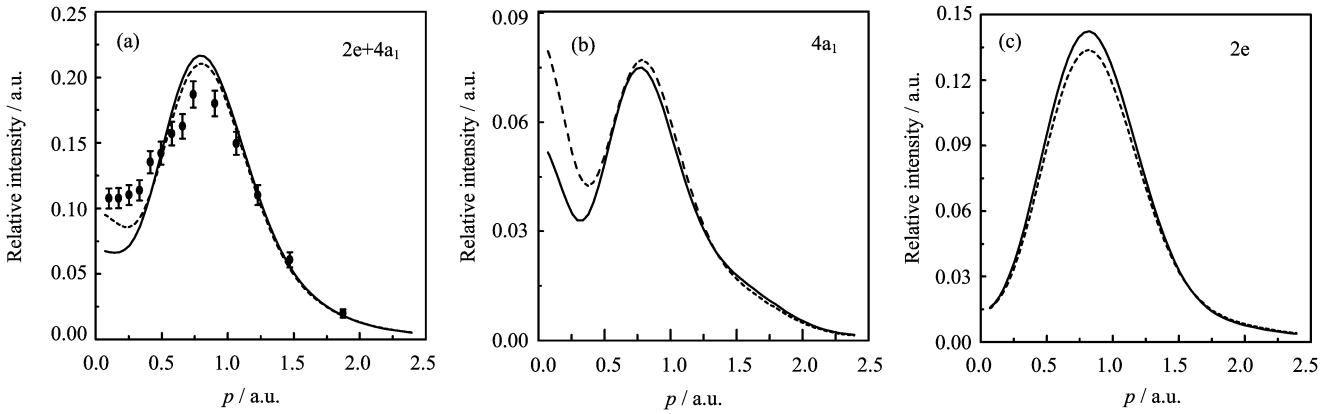

FIG. 3 Experimental and theoretical momentum profiles for the sum of 2e and $4a_1$ orbitals of $CFCl_3$, together with the TMPs for individual orbital. Experiment of this work (•), B3LYP/6-311++G** TMPs for neutral (solid line), and cationic (broken line) geometry.

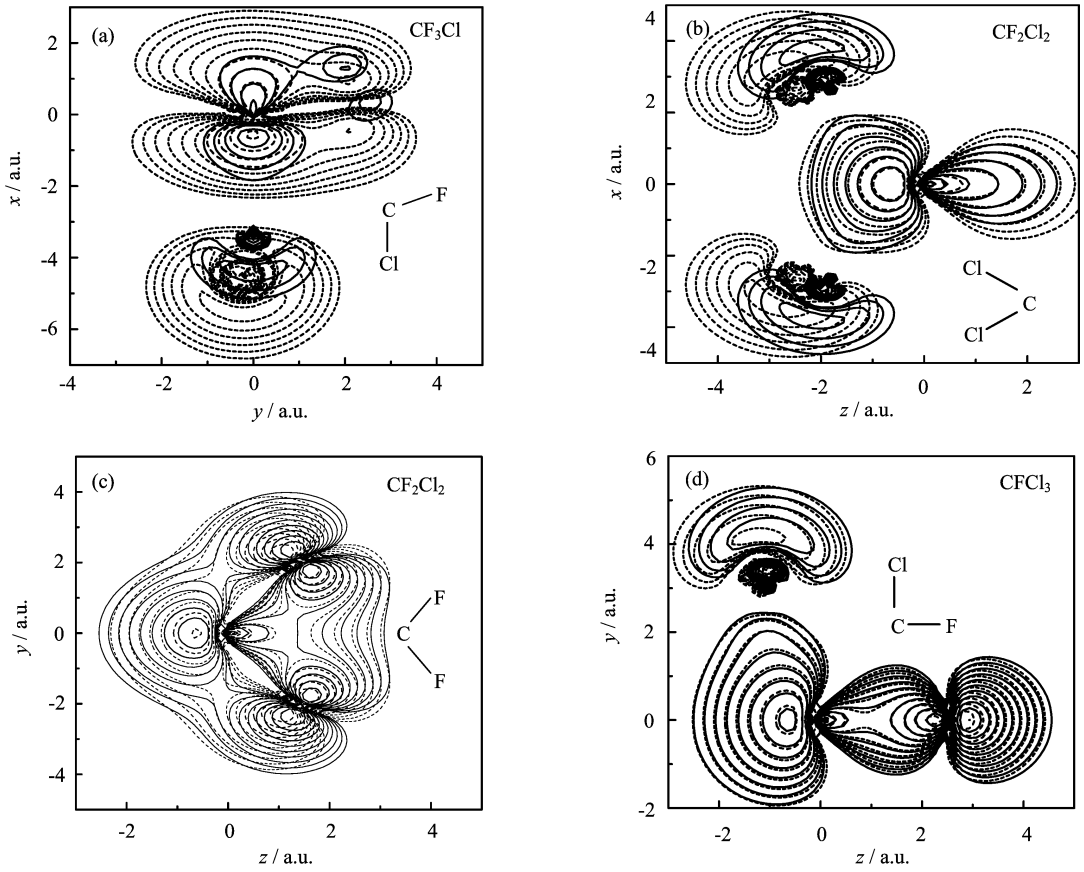

FIG. 4 Electron density contour maps for $4a_1$ orbitals of CF_3Cl, CF_2Cl_2, and $CFCl_3$ in the position space calculated using B3LYP with 6-311++G**. The solid curves and the dash curves represent the calculated results using the neutral geometry and the cationic geometry respectively. The contour values represent 63%, 40%, 25%, 16%, 10%, 6.3%, 2.5%, 1.6%, and 1% of the maximum density.

dicted by Jadrny *et al.* [35].

For CF_3Cl, as are shown in Fig.4(a), electron density distribution for $4a_1$ orbital in position space calculated using the cationic geometry is more diffuse than that calculated using the neutral geometry, especially for the part of Cl3s. According to the corresponding relation between momentum space and position space (Fourier transform), the diffusion of electron density distributions for cationic geometry in position space means the compression of electron momentum density towards the

DOI:10.1088/1674-0068/22/06/642-648

low momentum region. It can also be seen from Fig.1 that the peak of electron momentum distribution for cationic geometry slightly moves towards the low momentum region, which comes from the diffusion of C−F bonding electron density distribution in position space, while the high "turn up" in the low momentum region is mainly due to the diffusion of C−Cl bonding (mainly Cl3s) electron density distribution in position space.

For $4a_1$ orbital of CF_2Cl_2, as are shown in Fig.4 (b) and (c), C−Cl bonding electron density distribution in position space calculated in the cationic geometry is also more diffuse than that in the neutral geometry. In the light of Fourier transform from position space to momentum space, the high intensity in the low momentum region should be ascribed to the diffusion of C−Cl bonding electron density distributions in position space. As for $4a_1$ orbital of $CFCl_3$ shown in Fig.4(d), electron density distribution of C−Cl bond, especially near the nuclear region, exhibits some sort of diffusion. Hence, the high 'turn up' in the low momentum region should also be ascribed to the diffusion of C−Cl bonding electron density distribution in position space. Although the diffusion is not large, the improvement is still obvious in the low momentum region (in Fig.3) because $4a_1$ orbital of $CFCl_3$ possesses the contribution from three C−Cl bonds.

IV. CONCLUSION

In this work, we have investigated the origin of large discrepancies between TMPs and XMPs for $4a_1$ orbitals of CF_3Cl, CF_2Cl_2, and $CFCl_3$ molecules in low momentum region. The tentative calculations and further analyses show that the observed high intensity in low momentum region should be ascribed to the influence of molecular geometry change on C−Cl bonding electron density distributions of $4a_1$ orbitals, which is a positive evidence of molecular geometry distortion obtained by electron momentum spectroscopy. In order to explore the origin more exactly, further studies involving nuclear dynamics, distorted wave effects and electron correlation effects are desirable.

V. ACKNOWLEDGMENTS

This work was supported by the National Natural Science Foundation of China (No.10734040) and the Chinese Academy of Science Knowledge Promotion Project (No.KJCX1-YW-N30). The authors also gratefully acknowledge Professor C. E. Brion from University of British Columbia (UBC) in Canada for supplying the HEMS and RESFOLD programs.

[1] I. E. McCarthy and E. Weigold, Rep. Prog. Phys. **91**, 789 (1991).
[2] M. A. Coplan, J. H. Moore, and J. P. Doering, Rev. Mod. Phys. **66**, 985 (1994).
[3] C. E. Brion, Int. J. Quant. Chem. **29**, 1397 (1986)
[4] J. J. Neville, Y. Zheng, and C. E. Brion, J. Am. Chem. Soc. **118**, 10533 (1996).
[5] Y. Zheng, J. J. Neville, and C. E. Brion, Science **270**, 786 (1995).
[6] C. E. Brion, Y. Zheng, J. Rolke, J. J. Neville, I. E. McCarthy, and J. Wang, J. Phys. B: At. Mol. Opt. Phys. **31**, L223 (1998).
[7] J. Rolke, Y. Zheng, C. E. Brion, S. J. Chakravorty, E. R. Davidson, and I. E. McCarthy, Chem. Phys. **215**, 191 (1997).
[8] I. V. Litvinyuk, Y. Zheng, and C. E. Brion, Chem. Phys. **253**, 41 (2000).
[9] M. Takahashi, T. Saito, J. Hiraka, and Y. Udagawa, J. Phys. B: At. Mol. Opt. Phys. **36**, 2539 (2003).
[10] Y. Khajuria, M. Takahashi, and Y. Udagawa, J. Electron Spectrosc. Relat. Phenom. **133**, 113 (2003).
[11] X. G. Ren, C. G. Ning, J. K. Deng, S. F. Zhang, G. L Su, F. Huang, and G. Q. Li, Phys. Rev. Lett. **94**, 163201 (2005).
[12] J. A. Tossell, J. H. Moore, and M. A. Coplan, Chem. Phys. Lett. **67**, 356 (1979).
[13] M. P. Banjavčić, T. A. Daniels, and K. T. Leung, Chem. Phys. **155**, 305 (1991).
[14] R. R. Goruganthu, M. A. Coplan, J. H. Moore, and J. A. Tossell, J. Chem. Phys. **89**, 25 (1988).
[15] K. T. Leung, J. A. Sheehy, and P. W. Langhoff, Chem. Phys. Lett. **157**, 135 (1989).
[16] B. P. Hollebone, J. J. Neville, Y. Zheng, C. E. Brion, Y. Wang, and E. R. Davidson, Chem. Phys. **196**, 13 (1995).
[17] A. O. Bawagan, C. E. Brion, E. R. Davidson, and D. Feller, Chem. Phys. **113**, 19 (1987).
[18] P. Duffy, D. P. Chong, M. E. Casida, and D. R. Salahub, Phys. Rev. A **50**, 4707 (1994).
[19] Z. J. Li, X. J. Chen, X. Shan, T. Liu, and K. Z. Xu, J. Chem. Phys. **130**, 054302 (2009) and references therein.
[20] B. Hajgato, M. S. Deleuze, and F. Morini, J. Phys. Chem. A **113**, 7138 (2009) and references therein.
[21] X. J. Chen, C. K. Xu, C. C. Jia, Y. Khajuria, and K. Z. Xu, J. Phys. B: At. Mol. Opt. Phys. **34**, 4845 (2001).
[22] X. J. Chen, L. X. Zhou, X. H. Zhang, X. F. Yin, C. K. Xu, X. Shan, Z. Wei, and K. Z. Xu, J. Chem. Phys. **120**, 7933 (2004).
[23] L. X. Zhou, X. Shan, X. J. Chen, X. F. Yin, X. H. Zhang, C. K. Xu, Z. Wei, and K. Z. Xu, J. Electron Spectrosc. Relat. Phenom. **153**, 58 (2006).
[24] C. G. Ning, X. G. Ren, J. K. Deng, G. L. Su, S. F. Zhang, F. Huang, and G. Q. Li, Chin. Phys. **14**, 2467 (2005).
[25] X. Shan, X. J. Chen, L. X. Zhou, Z. J. Li, T. Liu, X. X. Xue, and K. Z. Xue, J. Chem. Phys. **125**, 154307 (2006).
[26] J. Rolke, Y. Zheng, C. E. Brion, Z. Shi, S. Wolfe, and E. R. Davidson, Chem. Phys. **244**, 1 (1999).
[27] J. Rolke, Y. Zheng, C. E. Brion, Y. A. Wang, and E. R. Davidson, Chem. Phys. **230**, 153 (1998).

DOI:10.1088/1674-0068/22/06/642-648

[28] J. Rolke, N. Cann, Y. Zheng, B.P. Hollebone, C. E. Brion, Y. A. Wang, and E. R. Davidson, Chem. Phys. **201**, 1 (1995).
[29] Y. Zheng, W. N. Pang, R. C. Shang, X. J. Chen, C. E. Brion, T. K. Ghanty, and E. R. Davidson, J. Chem. Phys. **111**, 9526 (1999).
[30] Y. Zheng, C. E. Brion, M. J. Brunger, K. Zhao, A. M. Grisogono, S. Braidwood, E. Weigold, S. J. Chakravorty, E. R. Davidson, A. Sgamellotti, and W. von-Niessen, Chem. Phys. **212**, 269 (1996).
[31] Y. Zheng, J. J. Neville, C. E. Brion, Y. Wang, and E. R. Davidson, Chem. Phys. **188**, 109 (1994).
[32] B. X. Yang, X. J. Chen, W. N. Pang, M. H. Chen, F. Zhang, B. L. Tian, and K. Z. Xu, Acta Phys. Sin. **5**, 862 (1997).
[33] V. G. Levin, V. G. Neudatchin, A. V. Pavlitchenkov, and Y. F. Smirnov, J. Chem. Phys. **63**, 1541 (1975).
[34] M. J. Frisch, G. W. Trucks, H. B. Schlegel, G. E. Scuseria, M. A. Robb, J. R. Cheeseman, V. G. Zakrzewski, J. A. Montgomery, Jr., R. E. Stratmann, J. C. Burant, S. Dapprich, J. M. Millam, A. D. Daniels, K. N. Kudin, M. C. Strain, O. Farkas, J. Tomasi, V. Barone, M. Cossi, R. Cammi, B. Mennucci, C. Pomelli, C. Adamo, S. Clifford, J. Ochterski, G. A. Petersson, P. Y. Ayala, Q. Cui, K. Morokuma, D. K. Malick, A. D. Rabuck, K. Raghavachari, J. B. Foresman, J. Cioslowski, J. V. Ortiz, B. B. Stefanov, G. Liu, A. Liashenko, P. Piskorz, I. Komaromi, R. Gomperts, R. L. Martin, D. J. Fox, T. Keith, M. A. Al-Laham, C. Y. Peng, A. Nanayakkara, C. Gonzalez, M. Challacombe, P. M. W. Gill, B. Johnson, W. Chen, M. W. Wong, J. L. Andres, C. Gonzalez, M. Head-Gordon, E. S. Replogle, and J. A. Pople, *Gaussian 98 Rev. A3*, Pittsburgh, PA: Gaussian Inc., (1998).
[35] R. Jadrny, L. Karlsson, L. Mattsson, and K. Siebahn, Phys. Scr. **16**, 235 (1977).

DOI:10.1088/1674-0068/22/06/642-648